Fuel 241 (2019) 451–458

Contents lists available at ScienceDirect

Fuel

journal homepage: www.elsevier.com/locate/fuel

Full Length Article

Study on the regenerable sulfur-resistant sorbent for mercury removal from nonferrous metal smelting flue gas

Zongwen Quan[a], Wenjun Huang[a], Yong Liao[a,b], Wei Liu[a], Haomiao Xu[a], Naiqiang Yan[a], Zan Qu[a,*]

[a] School of Environmental Science and Engineering, Shanghai Jiao Tong University, 800 Dong Chuan Road, Shanghai 200240, PR China
[b] Shanghai Institute of Pollution Control and Ecological Security, Shanghai 200092, PR China

GRAPHICAL ABSTRACT

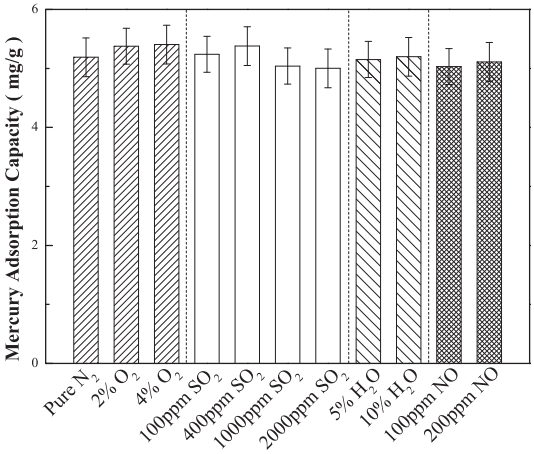

ARTICLE INFO

Keywords:
Mercury removal
Nonferrous smelting flue gas
Recycling
Sorbent
Regeneration

ABSTRACT

In order to remove and recycle elemental mercury from nonferrous smelting flue gas, cobalt sulfide sorbents were synthesized and tested. The mercury adsorption capacity of sorbent at 100 °C was 43.03 mg/g with 50% breakthrough threshold. The influences of the flue gas components and reaction temperature on the mercury adsorption capacity were investigated, respectively. The results shown that SO_2, H_2O, NO and O_2 had negligible impact on mercury adsorption of sorbents. Transmission electron microscopy (TEM), X-ray diffractometer (XRD), mercury programmed desorption (Hg-TPD) and X-ray photoelectron spectroscopy (XPS) were employed to characterize the sorbents. The mercury desorption activation energy from the sorbent was calculated based on a model built by the mercury temperature-programmed desorption data. Additionally, the used cobalt sulfide sorbent was regenerated. The results showed that the cobalt sulfide sorbent could maintain good adsorption performance after regeneration during several cycling tests. Therefore, cobalt sulfide is a suitable sorbent for the mercury removal and recycling from nonferrous metal smelting flue gas.

* Corresponding author.
E-mail address: quzan@sjtu.edu.cn (Z. Qu).

https://doi.org/10.1016/j.fuel.2018.12.040
Received 10 August 2018; Received in revised form 30 October 2018; Accepted 10 December 2018

1. Introduction

Mercury is one of the most world widely concerned pollutants due to its toxicity, bioaccumulation and persistence in the environment [1,2]. In order to protect human health and the environment, the *Minamata Convention on Mercury*, an international treaty entered into force on 16 August 2017. Among anthropogenic sources of mercury emissions, nonferrous metals smelting flue gas was considered as one of the primary sources [3]. The mercury emission from nonferrous metals smelter contributed about 38% to the anthropogenic atmospheric mercury in China [4]. Accordingly, reducing the mercury emission from nonferrous metal smelting flue gas is significant for the controlling of mercury pollution.

In the typical air pollutants control process for nonferrous metal smelter, the flue gas passes through the dust collector, wet scrubber and electrostatic demister successively to remove particles and SO_3 [5]. During this process, the particulate-bound mercury (Hg^p) and oxidized mercury (Hg^{2+}) could be removed by dust collector and wet scrubber, respectively. However, the absorbed Hg^{2+} will convert to Hg^0 and re-emit to the flue gas in the presence of sulfite during the SO_2 absorption. [6] While, it is difficult to remove the elemental mercury (Hg^0) because of its insolubility and high volatility [7]. Therefore, the difficulty of controlling mercury emission is removing Hg^0 from the flue gas.

Many technologies have been investigated for the removal of Hg^0 from coal-fired flue gas [8–13]. While, the mercury concentration in nonferrous metal smelting flue gas is about tens of milligrams per cubic meter, which is much higher than that in coal-fired flue gas [7]. Accordingly, these mercury removal technologies used in coal-fired flue gas may not suitable for the mercury removal from nonferrous metal smelting flue gas. Moreover, the high concentration mercury deserves to be recycled because of its commercial value. So, the mercury recycle method should be taken into account during the mercury removal from nonferrous metal smelting flue gas. Absorption technology and adsorption technology are the major technologies to remove mercury from nonferrous metal smelting flue gas. Among them, Boliden-Norzink process is a mature technology to absorb and recycle Hg^0 from nonferrous metal smelting flue gas. But, the mercury concentration in the outlet of Boliden–Norzink unit is still too high to meet the strict emission limitations [3]. Furthermore, the absorption technique is limited for widely application because of its high cost and corrosion problems [14]. Thus, adsorption technology seems more efficient to remove mercury from nonferrous metals smelting flue gas because it is simple, economical and effective [15,16]. Lots of sorbents, such as selenium sorbents and activated carbon sorbent have been applied to adsorb mercury from flue gas [17]. Nevertheless, the mercury adsorption capacities of these sorbents are not satisfied. Moreover, the high concentration SO_2 in flue gas will inhibit the mercury removal by sorbents [18]. Therefore, developing a novel high adsorption capacity and sulfur-resistant sorbent is meaningful for the mercury removal and recycling from nonferrous smelting flue gas.

In recent research, metal sulfides showed a fast reaction rate and high mercury adsorption performance to remove Hg^0 from coal-fired flue gas [19–22]. Meanwhile, these sulfide materials also showed good mercury removal efficiency in the presence of SO_2. Accordingly, the metal sulfide sorbent maybe a good choice for the mercury removal from nonferrous smelting flue gas containing high concentration SO_2. However, the metal sulfide sorbent was only tested in simulated coal-fired flue gas. How about its mercury removal performance in nonferrous metal smelting flue gas with high concentration mercury and SO_2? In the study, cobalt sulfide sorbents were synthesized and tested in fixed-bed adsorption system. It showed high mercury removal efficiency from simulated nonferrous metal smelting flue gas. The used cobalt sulfide sorbent could be regenerated and maintain high mercury removal performance during several cycling tests. It is a promising sorbent for the mercury removal and recycling from nonferrous metal smelting flue gas.

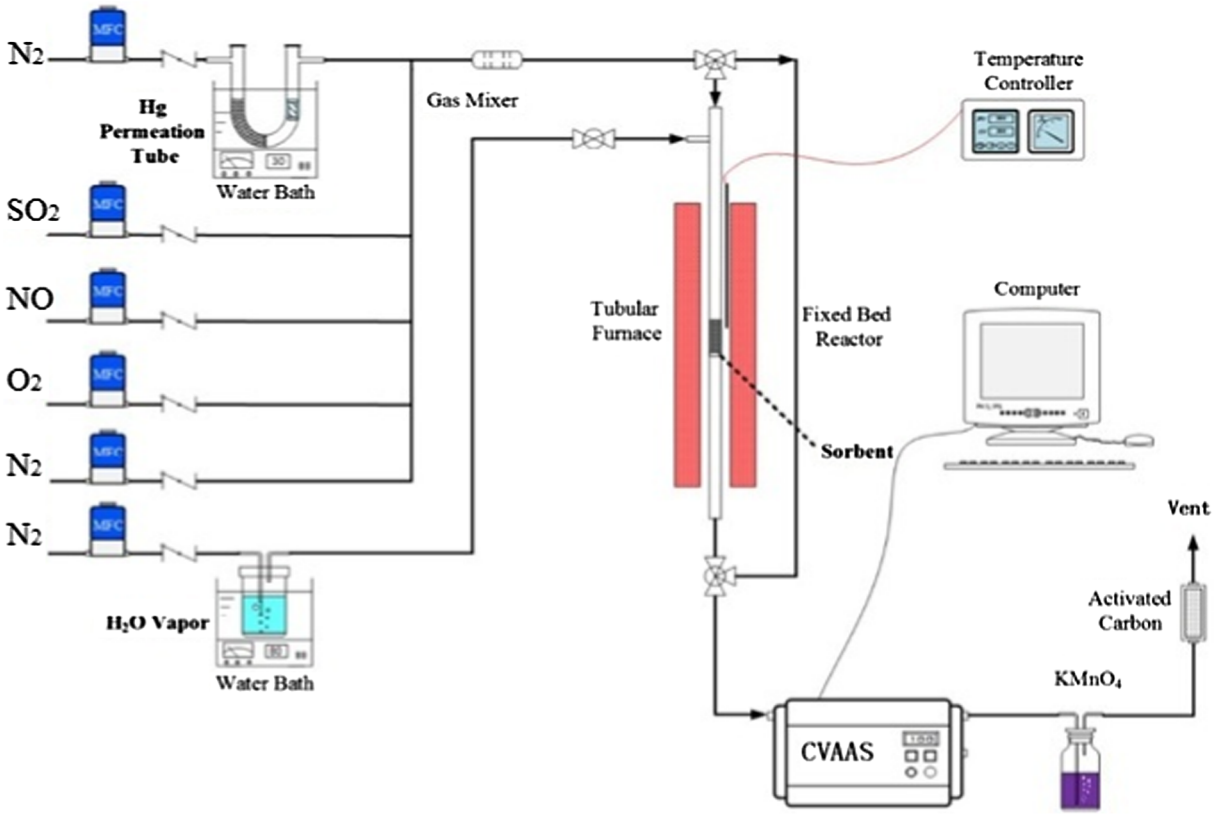

Fig. 1. The sketch of fixed-bed adsorption reaction system.

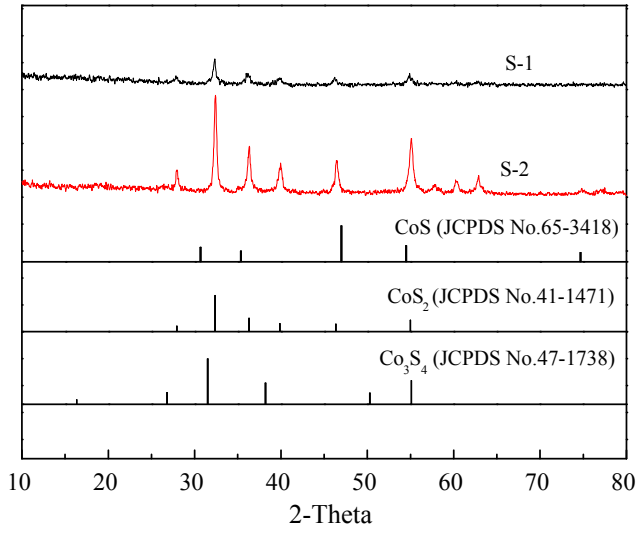

Fig. 2. XRD pattern of cobalt sulfide sorbents.

2. Experimental

2.1. Chemicals

The Chemicals used in this research were $Co(NO_3)_2{\cdot}H_2O$ (AR), $Na_2S_2O_3$ (AR), Na_2S (AR), CS_2 (AR), Ethanol absolute (AR) and Sublimed sulfur (AR). All of these chemicals were purchased from Sinopharm Chemical Reagent Co., Ltd.

2.2. Preparation and regeneration method of sorbent

The cobalt sulfide sorbents were prepared by hydrothermal synthesis method. Firstly, a certain amount of $Co(NO_3)_2{\cdot}6H_2O$ and $Na_2S_2O_3$ (or Na_2S) were dissolved in 100 mL ultrapure water. Secondly, the mixed solution was transferred to a 150 mL stainless steel autoclave and was placed in an oven at 150 °C for 12 h. After cooling for 3 h, the sorbent was washed by CS_2, ultrapure water and absolute ethanol, respectively. Then, the sorbent was vacuum-dried at 65 °C for 12 h. The cobalt sulfide sorbents synthesized by $Co(NO_3)_2/Na_2S$ and $Co(NO_3)_2/Na_2S_2O_3$ were marked as sorbent S-1 and S-2, respectively.

The regeneration method of used sorbent was as following: Firstly, 0.5 g powder sulfur was added into 10 mL ultrapure water. Secondly, the mixture solution was heated to 98 °C. Thirdly, the spent sorbent was impregnated in the hot mixture solution for 3 min. Then, the sorbent was separated from the mixture solution and washed by ultrapure water and ethanol absolute for three times. Finally, the regenerated sorbent was dried at 65 °C for 12 h in vacuum drying oven.

2.3. Adsorption performance test

The Hg^0 removal performance of sorbents was evaluated in a lab-scale adsorption experimental system. The adsorption system was made of gas distribution system, fixed-bed reactor, elemental mercury detection devices, and the tail gas treatment system (Fig. 1). The diameter of fixed-bed quartz tube reactor was 4 mm. A certain amount of sorbent was filled in the reactor. The flux of simulated flue gas was 500 mL/

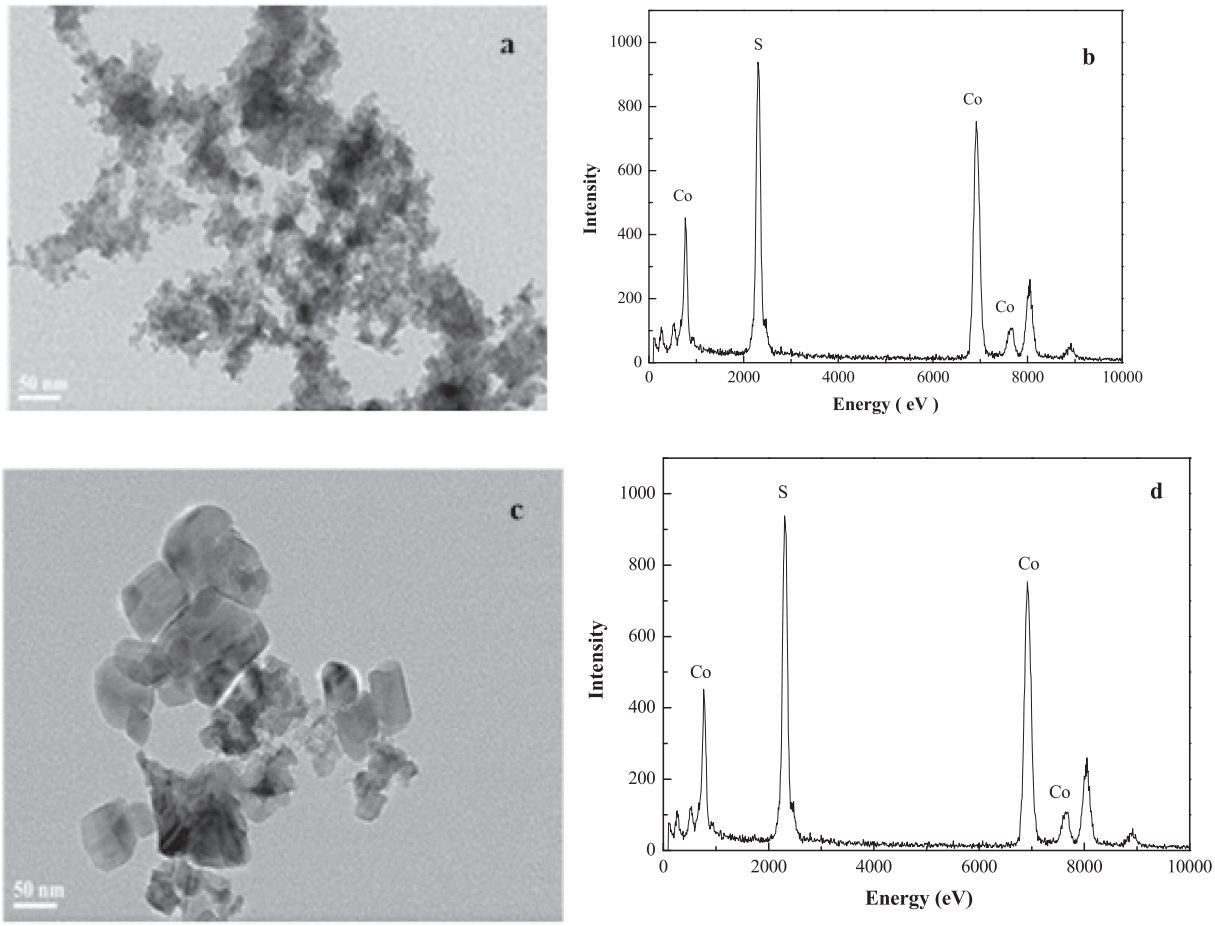

Fig. 3. TEM and EDX imagine of cobalt sulfide sorbent. a) TEM image of sorbent S-1, b) EDX image of sorbent S-1; c) TEM image of sorbent S-2; d) EDX image of sorbent S-2.

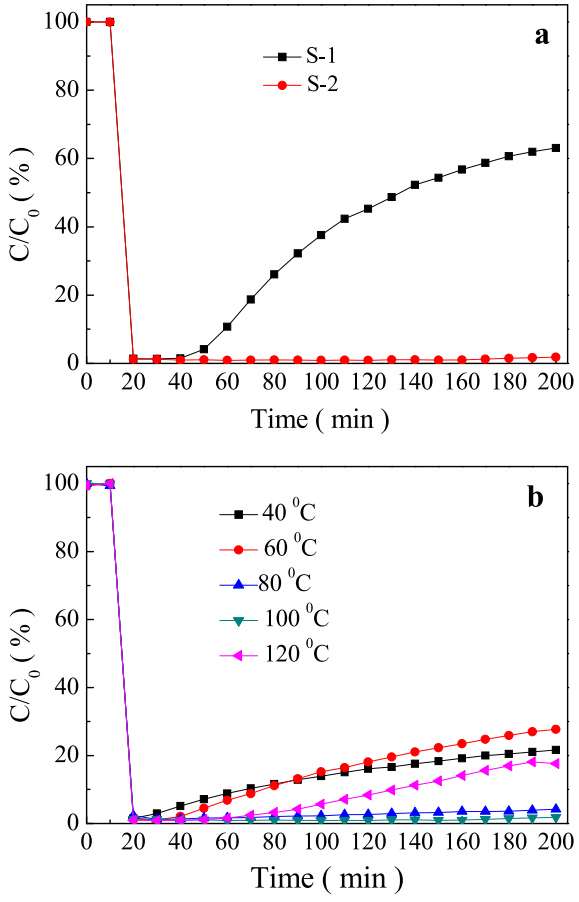

Fig. 4. The mercury adsorption performance of sorbents. a) mercury adsorption curve of sorbent S-1 and S-2; b) mercury adsorption curve of sorbent S-2 under different reaction temperature. Sorbent usage: 20 mg; Space velocity: $3.8 \times 10^5\,h^{-1}$; Mercury concentration: 1.3 mg/m^3; Reaction temperature: 40–120 °C; Carrier gas: N_2; Reaction time: 190 min; The flux of simulated flue gas was 500 mL/min; Sorbent size: 120 mesh (0.125 mm).

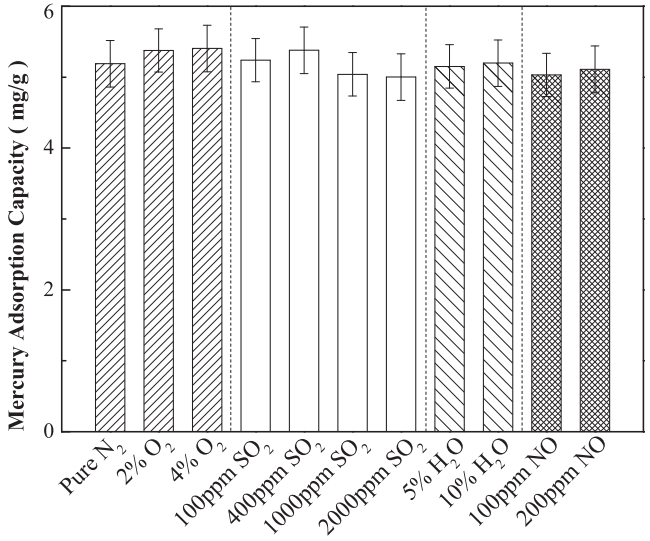

Fig. 5. Impact of SO_2, O_2 and H_2O on adsorption capacity of sorbent. Sorbent usage: 20 mg; Space velocity: $3.8 \times 10^5\,h^{-1}$; Mercury concentration: 1.3 mg/m^3; Reaction temperature: 100 °C; Carrier gas: N_2; Reaction time: 190 min; The flux of simulated flue gas was 500 mL/min; Sorbent size: 120 mesh (0.125 mm).

min. The gas space velocity was about $3.8 \times 10^5\,h^{-1}$. The elemental mercury concentration was about 1.3 ± 0.1 mg/m^3. The reactor temperatures could be adjusted from 30 to 350 °C by tubular furnace. In order to investigate the effects of flue gas components on mercury capture by sorbent, O_2, SO_2, NO and H_2O were introduced into the experimental system, respectively. The Hg^0 concentration was detected by a cold vapor atomic adsorption spectrometer mercury detector (CVASS) and verified by mercury analyzer (Lumex RA 915+, Russia). The elemental mercury removal efficiency and the adsorption capacity of sorbents were calculated by the followed equations:

$$\eta = \frac{Hg^0_{in} - Hg^0_{out}}{Hg^0_{in}} \times 100\% \quad (1)$$

$$Q = \frac{1}{m} \times \int_{t_0}^{t_1} (Hg^0_{in} - Hg^0_{out}) \times f \times dt \quad (2)$$

where η is the Hg^0 removal efficiency, Hg^0_{in} and Hg^0_{out} are the inlet concentration and outlet concentration of Hg^0, Q is the adsorption capacity, m is the mass of sorbents, f denotes the flow rate of the influent, and t_0 and t_1 represent the initial and ending test time of the breakthrough curves, respectively.

During desorption experiments of sorbent, spent sorbent was heated under the protective gas from 30 °C to 350 °C and stopped till the mercury signal decrease to the baseline level. The protective gas was high purity nitrogen and flow rate was controlled at 500 mL/min in this experiment.

2.4. Material characterization

The surface area of sorbents was detected by a surface area and pore size analyzer (Quantachrome Instruments NOVA 2200e). Specific surface areas were calculated through Brunauer-Emmmett-Teller (BET) method. The sorbents we synthesized were degassed at 120 °C for 2 h before the measurement. X-ray diffraction (XRD) patterns were performed by a Shimadzu XRD-6000 (40kv and 40 mA). The XRD data were tested at a scan rate of 10 degree per minute in the 2 theta range from 10° to 80°. Morphology observations and energy dispersive X-ray (EDX) analysis of the cobalt sulfide sorbent was characterized by transmission electron microscopy (TEM, JEM-2100). The mercury temperature-programed desorption (Hg-TPD) experiment was carried out in a temperature programmed furnace with different heating rate from 80 to 500 °C. The desorbed mercury was detected by CVAAS detector (SG921). The X-ray photoelectron spectroscopy (XPS) was performed on an X-ray photoelectron spectroscopy instrument (Thermo Fisher, 250Kl). And the binding energy of C 1 s was 284.6 eV used as a reference for the other elemental binding energy calibration.

3. Results and discussion

3.1. The characterization of sorbent

The structure of synthesized cobalt sulfide sorbent was shown in Fig. 2. As shown in Fig. 2, The XRD pattern of the cobalt sulfide sorbent didn't match well to the standard curve of CoS (JCPDS Card No. 65-3418), CoS_2 (JCPDS Card No. 41-1471), and Co_3S_4 (JCPDS Card No. 47-1738). The average size of particles for sorbent S-1 and S-2 calculated by using the Scherrer formula with all the reflection peaks were about 10–15 nm and 30–50 nm, respectively (Fig. 3a and c). The specific surface areas, pore volume and pore diameter of sorbents were 3.71 m^2/g (S-1), 23.56 m^2/g (S-2), 0.03 m^3/g (S-1), 0.36 m^3/g (S-2), 39.48 nm (S-1) and 53.49 nm (S-2), respectively. Chemical analysis using energy dispersive X-ray spectrometry (Fig. 3b and d) indicated the presence of Co and S in the sorbents and the atomic ratio of Co to S

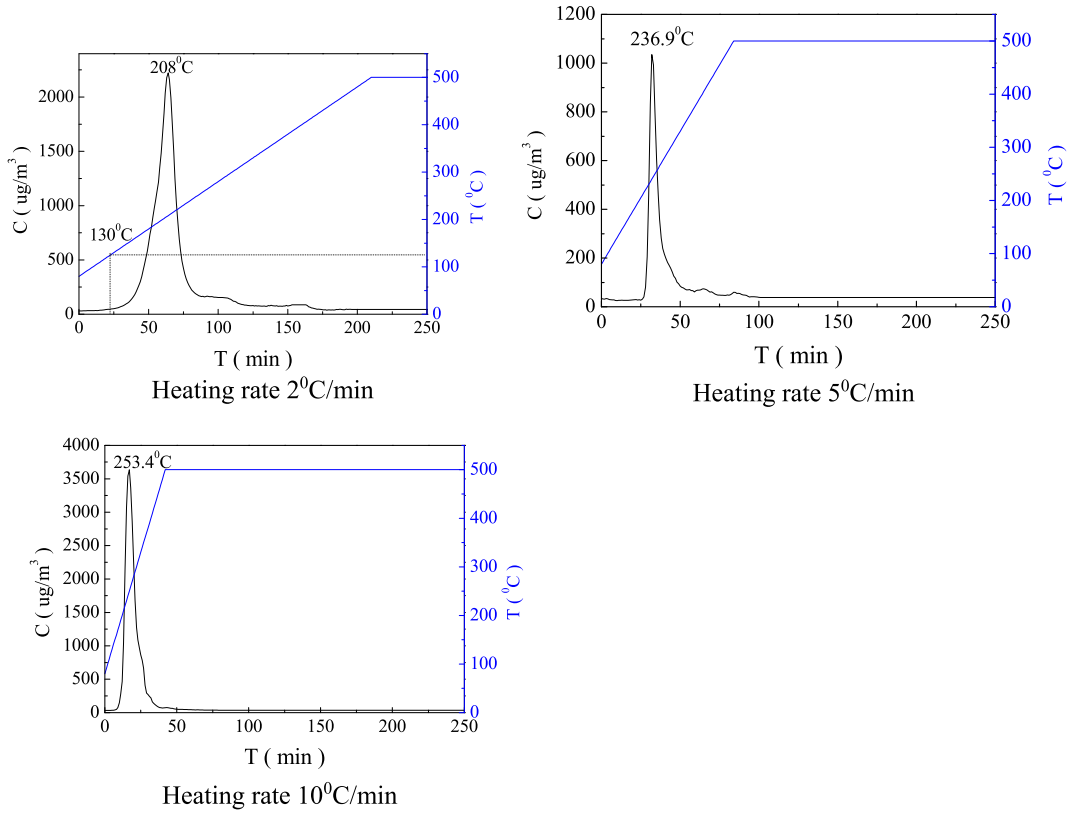

Fig. 6. Hg-TPD curves on sorbent at different heating rate. a) Heating rate: 2 °C/min; b) Heating rate: 5 °C/min; c) Heating rate: 10 °C/min. Adsorption condition: Sorbent usage: 10 mg; Space velocity: $1.9 \times 10^5\ h^{-1}$; Mercury concentration: 1.3 mg/m^3; Reaction temperature: 100 °C; Carrier gas: N_2; The flux of simulated flue gas was 500 mL/min; Reaction time: 60 min; Sorbent size: 120 mesh (0.125 mm). Desorption condition: Reaction temperature: 80–500 °C; Carrier gas: N_2; The flux of simulated flue gas was 700 mL/min; Reaction time: 250 min.

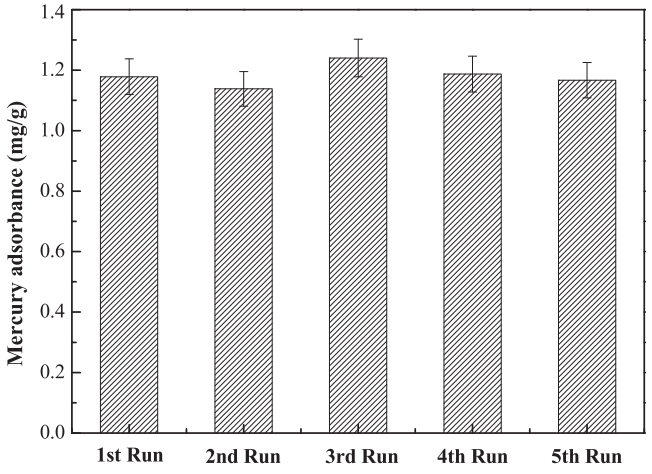

Fig. 7. Mercury adsorption capacities on sorbent in 5 cyclic tests. Sorbent usage: 100 mg; Space velocity: $7.6 \times 10^4\ h^{-1}$; Mercury concentration: 1.3 mg/m^3; Reaction temperature: 100 °C; Carrier gas: N_2; Reaction time: 190 min; The flux of simulated flue gas was 500 mL/min; Sorbent size: 120 mesh (0.125 mm).

is near to 1: 1.04 and 1:1.28, respectively. Thus, the major component of sorbent S-1 and S-2 may be CoS and Co_3S_4, respectively.

3.2. Hg^0 removal performance

The mercury removal performance of sorbent S-1 and S-2 were tested firstly. From the Fig. 4a, it could be seen that sorbent S-2 showed better mercury removal performance than sorbent S-1. Subsequently, the mercury removal performance of sorbent S-2 was evaluated at different reaction temperature. As shown in Fig. 4b, mercury removal efficiency of sorbent S-2 decreased remarkably with the increase of reaction time when the reaction temperature were 40, 60 and 120 °C, respectively. 100 °C was the optimal adsorption temperature for the mercury capture by sorbent S-2 in this research. The mercury removal efficiency could maintain about 98.2% at 100 °C even when the experiment time was 190 min. The mercury adsorption curve of sorbent S-2 was showed in Fig. S1. The mercury adsorption capacity of sorbent at 100 °C was 43.03 mg/g with 50% breakthrough threshold which was much higher than those reported mercury sorbents (Table S1) [19–22].

Table 1
The mole ratios of desorbed and adsorbed mercury in 5 cyclic experiments.

reaction	Q_d/Q_a (100%)
1st Run	97.4%
2nd Run	96.3%
3rd Run	95.0%
4th Run	97.1%
5th Run	96.0%

*Q_a: The amount of adsorbed mercury; Q_d: The amount of desorbed mercury.

3.3. Impact of flue gas components

The real nonferrous metal smelting flue gas is complex. In order to evaluate the mercury adsorption performance of sorbent S-2 in real nonferrous metal smelting flue gas, the influences of common components on mercury adsorption capacity of sorbent were investigated.

As shown in Fig. 5, the mercury adsorption capacity of sorbent S-2

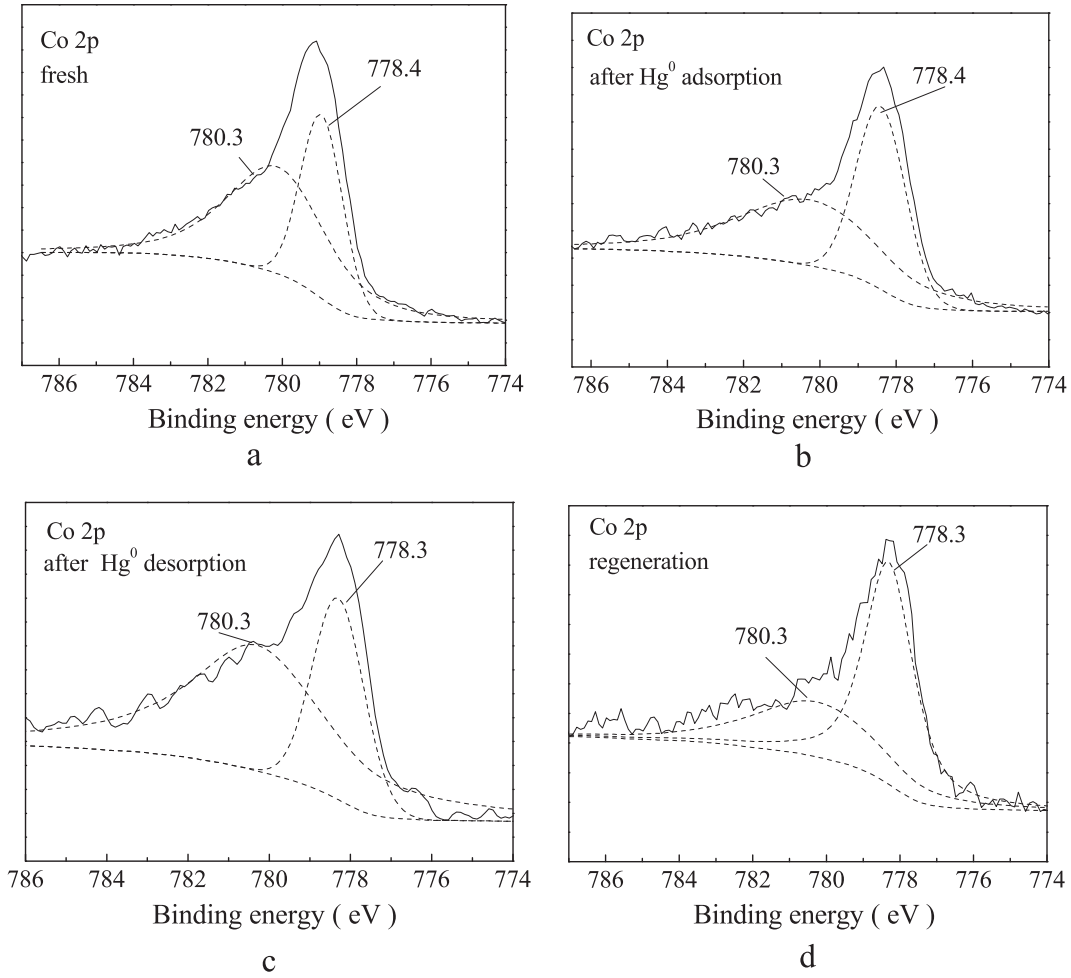

Fig. 8. XPS spectra of sorbent over Co 2p region. a) Co 2p on fresh sorbent; b) Co 2p on sorbent after adsorption; 3) Co 2p on sorbent after desorption at 350 °C; d) Co 2p on sorbent after regeneration.

Table 2
The mole ratio of cobalt spices in different sorbents.

Sample	Co^{3+}	Co^{2+}
Fresh Sorbent	63.8%	36.2%
Sorbent after adsorption	57.0%	43.0%
Sorbent after desorption	28.5%	71.5%
Sorbent after regeneration	61.8%	38.2%

was about 5.21 mg/g after 190 min adsorption reaction. When the SO_2 concentration increased from 1000 ppm to 2000 ppm, the mercury adsorption capacities were about 5.1 and 5.0 mg/g, respectively. It meant that the presence of SO_2 had little impact on Hg^0 adsorption by sorbent S-2. Meanwhile, no remarkable differences were observed when the concentration of O_2, NO and H_2O were changed. This indicated O_2, NO and H_2O didn't affect the mercury adsorption capacity of sorbent S-2.

3.4. Mercury desorption

A serial of Hg-TPD experiments were carried out to investigate the mercury desorption performance of sorbent. The used cobalt sorbent was heated into furnace under different heating rated and the mercury desorption curves was shown in Fig. 6. It could be found that one peak emerged during the desorption process, which indicated that there was only one adsorption sites on the sorbent's surface. As shown in Fig. 6a, the adsorbed mercury began to desorb at 130 °C. The amount of released mercury was about 0.04 mg which was about 97.4% of the mercury amount adsorbed by sorbent S-2. Therefore, the adsorbed mercury could be recycled easily by heating. But the mercury adsorption performance of used sorbent after desorption was not satisfied (Fig. S2).

From the Fig. 6, it also could be seen that the peak positions were different with the change of heating rate. A model was built for evaluation of mercury desorption activation energy based on the temperature programmed desorption data. The energy could be calculated according to Eq. (3) [23–25].

$$2\ln T_p - \ln\beta = \frac{E_d}{RT_p} + \ln\frac{E_d}{AR} \quad (3)$$

where T_p (K) represents the temperature at which the desorption rate reaches the maximum value, β (K·min^{-1}) is the heating rate, E_d is the desorption activation energy (kJ/mol), R is gas constant, A is pre-exponential factor. According to the calculation, the mercury desorption activation energy was about 63.9 kJ/mol (Table S2).

3.5. Mercury regeneration research

The used sorbent was treated by hot sulfur solution for regeneration. Then, the regenerated sorbent was tested again. 5 cycles of mercury adsorption, desorption and regeneration tests were performed in fixed-bed reactor. As shown in Fig. 7, there was no obvious difference between the mercury adsorption capacity of the fresh sorbent and regenerated sorbent. The mercury adsorption curves were also very close

in 5 cycles experiments (Fig. S3). That meant the adsorption rate and capacity of sorbent could be recovered after regeneration. Furthermore, over 95% adsorbed mercury could release from the used sorbent after 5 cycles experiments by heat treatment (Table 1). Thus, the sorbent S-2 could be used as a regenerable sorbent for the mercury capture and recycle from nonferrous metal smelting flue gas. In order to investigate the impact of elemental sulfur on mercury adsorption during the regeneration of sorbent, the mercury capture performance of Al_2O_3 was tested after the same treatment by hot sulfur solution. As showed in Fig. S4, the mercury adsorption performances of Al_2O_3 were very poor before and after treated by hot sulfur solution. Obviously, the reason why used sorbent S-2 could be recovered was not the action of elemental sulfur.

3.6. Hg^0 adsorption mechanism

To investigate the adsorption reaction mechanism of mercury removal by cobalt sulfide sorbent, the sorbents at different reaction time was tested by XPS. The XPS analysis of Co 2p for the fresh, used and regenerated cobalt sulfide sorbents were showed in Fig. 8. The ratios of cobalt spices at different conditions were summarized in Table 2.

As shown in Fig. 8, two main peaks corresponding to Co^{2+} (at 780.3 eV) and Co^{3+} (at 778.4 eV) were observed for all samples [26,27]. The sorbent S-2 maybe a mixture composed of Co_2S_3 and CoS. The XPS spectrum of Co 2p was changed after Hg^0 adsorption, which indicating the cobalt spices changed after adsorption reaction. According to the Table 2, it could be seen that the mole ratio of Co^{3+} decreased from 63.8% to 57.0% after mercury adsorption. While, the mole ratio of Co^{2+} increased from 36.2% to 43.0%. Moreover, the mole ratio of Co^{3+} increased to 61.8% after regeneration. It could be seen that the mercury removal performance was better when the mole ratio of Co^{3+} was higher. It indicated that Co^{3+} was the key of Hg^0 adsorption over cobalt sulfide sorbent. Part of Co^{3+} reacted with mercury and generated Co^{2+} after mercury adsorption. Meanwhile, Co^{2+} could be converted to Co^{3+} after regeneration of sorbent S-2. From the Fig. S5 the peaks of Hg 4f spectra over used sorbent centered at 101.0 and 105.1 eV were assigned to surface HgS. And there is no obvious difference between the S 2p spectra over the fresh and used sorbent. That meant there is no change on the sulfur of sorbent.

According to the above discussion, the Hg^0 adsorption process could be deduced as follows: Firstly, gaseous Hg^0 was adsorbed on the cobalt sulfide sorbent and formed Hg(ad). Then, Co^{3+} reacted with Hg(ad) to form HgS. And the reactions can be described as follows:

$$Hg^0_g + sorbent \rightarrow Hg^0_{ad} \quad (a)$$

$$Hg^0_{ad} + 2Co^{3+} \rightarrow 2Co^{2+} + HgS \quad (b)$$

According to the reaction (b), two mole Co^{3+} were reduced to Co^{2+} when one mole Hg^0 was converted to HgS. The mole ratio of Co^{3+} and Co^{2+} in fresh sorbent was 63.8%:36.2%. According to the calculation, the mercury adsorption capacity of cobalt sulfide sorbent for mercury was about 80.04 $mg \cdot g^{-1}$ after 24 h adsorption. Theoretically, the mole ratio of Co^{3+} and Co^{2+} in used sorbent should be 55.6%:44.4%. The data was very close to the XPS analysis results (Table 2, Co^{3+}/Co^{2+} = 57.0%:43%). It was very possible that the cobalt sulfide sorbent was a mixture composed of Co_2S_3 and CoS. And Co_2S_3 played the major role in the mercury capture.

4. Conclusions

Cobalt sulfide sorbents were successfully synthesized for the mercury capture from nonferrous metal smelting flue gas. It showed high mercury adsorption capacity and sulfur-resistant ability. The adsorbed mercury could be easily recycled from the sorbent by heating. And the sorbent could be regenerated and recycle utilized. Furthermore, the common components of nonferrous metal smelting flue gas, such as O_2, NO, H_2O and SO_2, have no inhibition effect on the removal of Hg^0 by cobalt sulfide sorbent. The above results show that cobalt sulfide sorbent can be a promising sorbent for removing and recycling Hg^0 from nonferrous metal smelting flue gas.

Acknowledgements

This study was supported by the National Key Research and Development Program of China (No. 2017YFC0210500) and the National Natural Science Foundation of China (No. 21677096) and (U1662132).

Appendix A. Supplementary data

Supplementary data to this article can be found online at https://doi.org/10.1016/j.fuel.2018.12.040.

References

[1] Wu YH, Xu WQ, Yang Y, Wang J, Zhu TY. Support effect of Mn-based catalysts for gaseous elemental mercury oxidation and adsorption. Catal Sci Technol 2018;8(1):297–306.
[2] Du BY, Feng XB, Li P, Yin RS, Yu B, Snoke JE, et al. Use of mercury isotopes to quantify mercury exposure sources in inland populations, China. Environ Sci Technol 2018;52(9):5407–16.
[3] Wang SX, Song JX, Li GH, Wu Y, Zhang L, Wang Q, et al. Estimating mercury emissions from a zinc smelter in relation to China's mercury control policies. Environ Pollut 2010;158(10):3347–53.
[4] Chen K, Wang Y, Tian HZ, Gao X, Zhang YX, Wu XC, et al. Atmospheric emission characteristics and control policies of five precedent-controlled toxic heavy metals from anthropogenic sources in China. Environ Sci Technol 2015;49:1206–14.
[5] Zhang L, Wang SX, Wu QR, Meng Y, Yang H, Wang FY, et al. Were mercury emission factors for Chinese non-ferrous metal smelters overestimated? Evidence from onsite measurements in six smelters. Environ Pollut 2012;171:109–17.
[6] Wang LD, Qi TY, Hu MX, Zhang SH, Xu PY, Qi D, et al. Inhibiting mercury re-emission and enhancing magnesia recovery by cobalt-loaded carbon nanotubes in a novel magnesia desulfurization process. Environ Sci Technol 2017;51(19):11346–53.
[7] Ma YP, Qu Z, Xu HM, Wang WH, Yan NQ. Investigation on mercury removal method from flue gas in the presence of sulfur dioxide. J Hazard Mater 2014;279:289–95.
[8] Wang T, Wu JW, Zhang YS, Liu J, Sui ZF, Zhang HC, et al. Increasing the chlorine active sites in the micropores of biochar for improved mercury adsorption. Fuel 2018;229:60–7.
[9] Tang L, Li CT, Zhao LK, Gao L, Du XY, Zeng JW, et al. A novel catalyst CuO-ZrO_2 doped on Cl- activated bio-char for Hg^0 removal in a broad temperature range. Fuel 2018;218:366–74.
[10] Wang FM, Shen BX, Gao LJ, Yang JC. Simultaneous removal of NO and Hg-0 from oxy-fuel combustion flue gas over CeO_2-modified low-V_2O_5-based catalysts. Fuel Process Technol 2017;168:131–9.
[11] Hao RL, Yang F, Mao XZ, Mao YM, Zhao Y, Lu YJ. Emission factors of mercury and particulate matters, and in situ control of mercury during the co-combustion of anthracite and dried sawdust sludge. Fuel 2018;230:202–10.
[12] Huang WJ, Qu Z, Chen WM, Xu HM, Yan NQ. An enhancement method for the elemental mercury removal from coal-fired flue gas based on novel discharge activation reactor. Fuel 2016;171:59–64.
[13] Wang QF, Liu Y, Wu ZB. Laboratory study on mercury release of the gypsum from the mercury co-removal wet flue gas desulfurization system with additives. Energy Fuels 2018;32(2):1005–11.
[14] Hylander LD, Herbert RB. Global emission and production of mercury during the pyrometallurgical extraction of nonferrous sulfide ores. Environ Sci Technol 2008;42(16):5971–7.
[15] Zhou Q, Duan YF, Chen M, Liu M, Lu P, Zhao SL. Effect of flue gas component and ash composition on elemental mercury oxidation/adsorption by NH4Br modified fly ash. Chem Eng J 2018;345:578–85.
[16] Yang ZQ, Li HL, Feng SH, Li P, Liao C, Liu X, et al. Multiform sulfur adsorption centers and copper-terminated active sites of nano-CuS for efficient elemental mercury capture from coal combustion flue gas. Langmuir 2018;34(30):8739–49.
[17] Ralston N. Nanomaterials: nano-selenium captures mercury. Nat Nanotechnol 2008;3(9):527–8.
[18] Presto AA, Granite EJ. Impact of sulfur oxides on mercury capture by activated carbon. Environ Sci Technol 2007;41(18):6579–84.
[19] Xu HM, Yuan Y, Liao Y, Xie JK, Qu Z, Shangguan WF, et al. $[MoS_4]^{2-}$ cluster bridges in Co−Fe layered double hydroxides for mercury uptake from S−Hg mixed flue gas. Environ Sci Technol 2017;51:10109–16.
[20] Li HL, Feng SH, Liu Y, Shih KM. Binding of mercury species and typical flue gas components on ZnS(110). Energy Fuels 2017;31:5355–62.
[21] Liao Y, Chen D, Zou SJ, Xiong SC, Xiao X, Dang H, et al. Recyclable naturally derived magnetic pyrrhotite for elemental mercury recovery from flue gas. Environ Sci Technol 2016;50:10562–9.

[22] Zhao HT, Yang G, Gao X, Pang CH, Kingman SW, Wu T. Hg^0 capture over CoMoS/γ-Al_2O_3 with MoS_2 nanosheets at low temperatures. Environ Sci Technol 2016;50:1056–64.
[23] Liu Y, Kelly DJA, Yang HQ, Lin CCH, Kuznicki SM, Xu ZG. Environ Sci Technol 2008;42:6205–10.
[24] Dong J, Xu ZH, Kuznicki SM. Environ Sci Technol 2009;43:3266–71.
[25] Yang SJ, Guo YF, Yan NQ, Wu DQ, He HP, Xie JK, et al. Appl Catal, B 2011;101:698–708.
[26] Liotta LF, Carlo GD, Pantaleo G, Venezia AM, Deganello G. Co_3O_4/CeO_2 composite oxides for methane emissions abatement: relationship between Co_3O_4–CeO_2 interaction and catalytic activity. Appl Catal, B 2006;66:217–27.
[27] Zhang AC, Zheng WW, Song J, Hu S, Liu ZC, Xiang J. Cobalt manganese oxides modified Titania catalysts for oxidation of elemental mercury at low flue gas temperature. Chem Eng J 2014;236:29–38.